Localized Structures and Localized Patterns in Optical Bistability

M. Tlidi, Paul Mandel, and R. Lefever
Faculté des Sciences, Université Libre de Bruxelles, Campus Plaine C.P. 231, B-1050 Bruxelles, Belgium
(Received 2 August 1993; revised manuscript received 20 April 1994)

We study numerically a Swift-Hohenberg equation describing, in the weak dispersion limit, nascent optical bistability with transverse effects. We predict that stable localized structures, and organized clusters of them, may form in the transverse plane. These structures consist of either kinks or dips. The number and spatial distribution of these localized structures are determined by the initial conditions while their peak (bottom) intensity remains essentially constant for fixed values of the system's parameters.

PACS numbers: 42.65.Pc, 42.60.Mi

At the onset of optical bistability, there is a critical point where the output versus input characteristics have an infinite slope. The vicinity of this critical point is characterized by critical slowing down [1]. This implies that the dynamics of the system is dominated by a characteristic decay time which is of geometrical origin. It is inversely proportional to the deviation from the critical point and diverges at criticality. Thus in the vicinity of the critical point, all atomic and cavity decay times are associated with fast decays. Let (X, Y, C) be the deviations of the cavity field, of the injected field, and of the cooperativity parameter with respect to the values of these quantities at the critical point:

$$Y_c = 3\sqrt{3}(1+\Delta^2)\ , \qquad X_c = \sqrt{3}(1+i\Delta),$$
$$C_c = 4(1+\Delta^2). \tag{1}$$

In these expressions, $\Delta \equiv (\omega_a - \omega_e)/\gamma_\perp = -\theta \equiv -(\omega_c - \omega_e)/\kappa$, where ω_a (ω_e, ω_c) is the atomic (external, cavity) frequency while $\gamma_\perp$ and κ are the atomic polarization and cavity decay rates. It has been demonstrated recently [2] that in the double limit of weak dispersion ($|\Delta| \ll 1$) and nascent bistability ($|C| \ll 1$), the spatiotemporal evolution of the electric field X obeys an equation of the Swift-Hohenberg type:

$$\frac{\partial X}{\partial t} = 4y + X(C - X^2) - 4\Delta\mathcal{L}_\perp X - \frac{4}{3}\mathcal{L}_\perp\mathcal{L}_\perp X, \tag{2}$$

where t is a dimensionless time, $y = Y - \frac{\sqrt{3}C}{2}$, and $\mathcal{L}_\perp$ is the transverse part of the Laplacian. Though this kind of equation is well known as a (variational) model for the near threshold dynamics of some hydrodynamical instabilities, its relevance in nonlinear optics has only been established recently [2]. The purpose of this Letter is to use Eq. (2) to predict the occurrence of stable stationary localized structures in optical devices in the vicinity of C_c. These structures consist of *kinks* (or *dips*) in the amplitude of the cavity field. They may either be spatially independent and randomly distributed or occur in clusters forming well-defined spatial patterns. We find that kinks and dips are also bistable when the homogeneous steady state solutions of (2) exhibit bistability. None of these structures has yet been found for a Swift-Hohenberg equation [3], though some of them have been reported for other (nonvariational) models studied in chemistry and hydrodynamics [4,5], and for the complex Ginzburg-Landau equation [6–9]; see [10], for a review on this topic.

The situation which interests us requires that $\Delta > 0$ (or equivalently that $\omega_a > \omega_e > \omega_c$). Notably, in that case, the transverse Laplacian term in (2) is destabilizing and allows for the formation of stationary, spatially periodic patterns characterized by an *intrinsic wavelength* solely determined by dynamical parameters and not by the system's physical dimensions or geometrical constraints (Turing instability, [11]). Using the η expansion, based on the distance from the Turing bifurcation point as the smallness parameter [12], we have analytically determined the variety and the stability properties of the patterns which are solutions of Eq. (2) in the weakly nonlinear regime where the Turing bifurcation is supercritical [13]. This analysis restricted the values of the cooperativity parameter to the range

$$C < -\frac{87\Delta^2}{38} \equiv C_{\text{sub}}\ , \tag{3}$$

in which, furthermore, the homogeneous steady states necessarily are monostable, whatever the value of the input field y is. We proved that under those conditions, the only stable patterns forming in bidimensional transverse systems are those which either have the hexagonal symmetry or consist of stripes. The results reported below describe the behaviors predicted on the basis of Eq. (2) for $C_{\text{sub}} < C$, i.e., in the strongly nonlinear regime where the Turing bifurcation is subcritical, and where the homogeneous steady states may be monostable ($C_{\text{sub}} < C < 0$) or bistable ($0 < C$). They are obtained by integrating (2) numerically for periodic boundary conditions, with a pure implicit Euler scheme supplemented by a finite difference method [13].

We first examine the case of a one-dimensional monostable system [cf. Fig. 1(a)]. The homogeneous steady states X_s undergo a Turing bifurcation either at y_{T-} when the input field is increased from below or at y_{T+} when it is decreased from above. Accordingly, in the

0031-9007/94/73(5)/640(4)$06.00

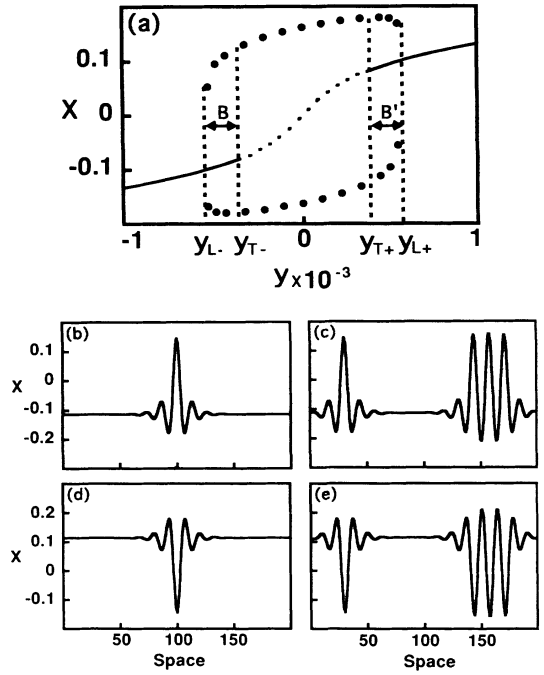

FIG. 1. 1D bifurcation diagram and localized structures in the monostable case ($\Delta = 0.1$, $C = -0.001$). (a) The full and broken lines correspond, respectively, to the stable and unstable homogeneous steady state solutions. The circles indicate the maximum (minimum) amplitude of the Turing solutions. (b) Single localized structure obtained after perturbing the stable homogeneous steady state in the subcritical region at one grid point ($y = -0.0004$, amplitude of the perturbation $\Delta X = 5$). (c) Localized pattern obtained after perturbing the homogeneous steady state at three grid points ($y = 0.0004$, $\Delta X = 5$). (d) The homogeneous steady state is perturbed at one grid point ($\Delta X = -5$, $y = 0.0004$). (e) The homogeneous steady state is perturbed at three grids points ($\Delta X = -5$, $y = 0.0004$).

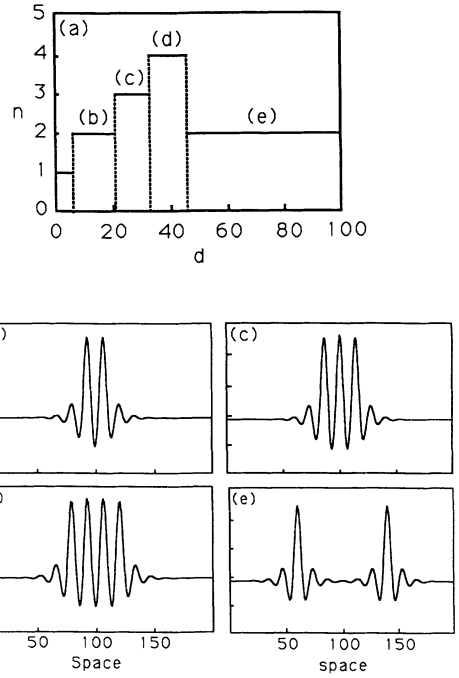

FIG. 2. (a) Number n of localized structures obtained after two perturbations are applied at two grid points separated by a distance d. (b)–(e) Localized structures obtained for different values of d ($y = 0.0004$, $\Delta X = 5$).

range

$$y_{T-} < y < y_{T+}$$

with

$$y_{T\pm} = \frac{3\Delta^2 - 2C}{12} X_{T\pm}, \quad X_{T\pm} = \pm\sqrt{\Delta^2 + \frac{C}{3}}, \qquad (4)$$

there exists a finite band of Fourier modes k,

$$k_-^2 < k^2 < k_+^2$$

with

$$k_\pm^2 = -\frac{3\Delta \pm \sqrt{3(3\Delta^2 - 3X_s^2 + C)}}{2}, \qquad (5)$$

which are linearly unstable and trigger the spontaneous evolution of X towards a stationary, spatially periodic distribution which occupies the whole of the cavity space available in the transverse direction. This solution is of finite amplitude [represented by full dots in Fig. 1(a)] in its entire domain of existence and stability. For y, this corresponds to the interval $y_{L-} < y < y_{L+}$. At the turning points $y = y_{L\pm}$, it connects with the unstable periodic solutions [not represented in Fig. 1(a)] branching off from the homogeneous steady states at $y = y_{T\pm}$. The existence of the latter is obviously restricted to y values lying in the subcritical domains B and B'.

Figures 1(b)–1(e) illustrate a remarkable property of the domains B and B', namely, that they are regions where the system exhibits *multistability*: besides the homogeneous steady states and the Turing patterns, which are both stable, an additional variety of stable patterns can be obtained. These *localized structures* are specific of B and B' in that they consist of kinks, as in Fig. 1(b), or of dips, as in Fig. 1(d), which join the Turing branch of bifurcated states [cf. dots in Fig. 1(a)] to the stable homogeneous steady states. The number and spatial distribution of kinks (or dips) immersed in the bulk of the basic homogeneous state depend on the initial conditions considered. Their peak (bottom) intensity remains, however, essentially constant for fixed values of the system's parameters. These features are exemplified in Fig. 1(c) [1(e)], which is obtained for the same values of the parameters as Fig. 1(b) [1(d)], but with a different initial condition. In Fig. 2, we see how the number of peaks obtained after two identical, largely suprathreshold, per-

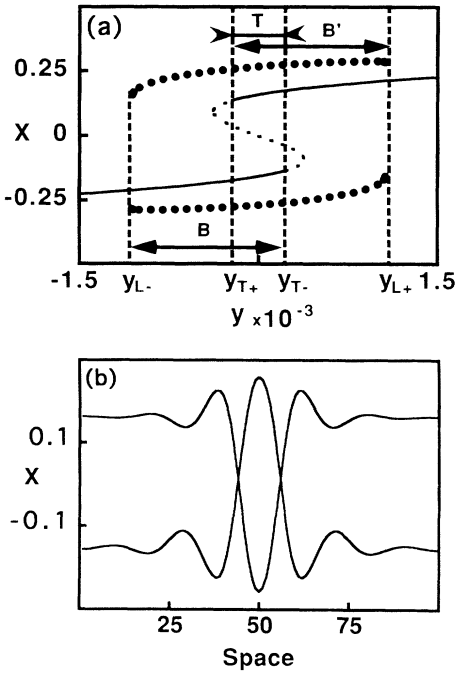

FIG. 3. 1D bifurcation diagram and localized structures in the bistable case ($\Delta = 0.1$, $C = 0.025$). (a) The full and broken lines correspond, respectively, to the stable and unstable homogeneous steady state solutions. The circles indicate the maximum (minimum) amplitude of the Turing solutions. (b) Coexistence of kink and dip for $y = 0$. Depending on the initial condition, the system evolves to either one of these solutions. It is worthwhile to stress that the domain of coexistence between kinks and dips is not restricted to the value $y = 0$, but extends to the entire range for which B and B' overlap, i.e., the domain labeled T.

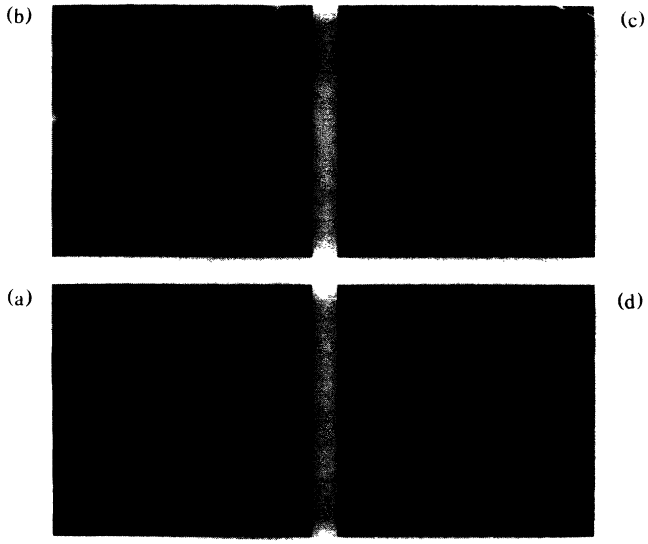

FIG. 4. Localized structures and patterns with two transverse dimensions ($\Delta = 0.1$, $C = 0.025$, and $y = -0.0005$). (a) Single localized structure ($\Delta X = 5$, 60×60 grid). (b) Random distribution of localized structures; the system is perturbed by small amplitude ($X = 0.92$, $\Delta X = 0.05$, 60×60 grid). (c) Localized pattern (centered hexagons). The steady state is perturbed at seven grid points. (d) Localized pattern (three centered hexagons, 100×100 grid).

turbations of the homogeneous steady state depends on the distance d between them. The parameters have the same values as in Fig. 1, which corresponds for the Turing patterns to a wavelength $\Lambda \approx 13.5$. As reported in Figs. 2(a)–2(d), the number n of kinks observed in the localized structure reached for $t \to \infty$ is, up to $n = 4$, approximately given by the relation $n = d/\Lambda$. Thus, if $d \lesssim 45$, the evolution of the perturbations is strongly correlated which leads to localized patterns in which up to four peaks develop and remain clustered together. If d increases further, the perturbations evolve independently and the final pattern simply consists of two peaks whose localization corresponds to that of the two initial perturbations.

Similar behaviors are found when the homogeneous steady states exhibit bistability, i.e., when $0 < C$ (cf. Fig. 3). In addition, however, in that part of the bistable domain where B and B' overlap [labeled T in Fig. 3(a)], kinks and dips exibit bistability [see Fig. 3(b)]. In other words, under those conditions, five distinct kinds of steady states are stable: the upper and lower branches of homogeneous steady states, the Turing patterns, and the upper (dips) and lower (kinks) localized patterns.

In 2D, the set of localized solutions is necessarily much larger. A single localized structure is shown in Fig. 4(a). Figure 4(b) shows that the final stable solution, which is obtained with an initially random distribution of amplitudes, displays a random distribution of localized structures. More interesting is the emergence of localized patterns, which are organized clusters of localized structures. We find that the centered hexagon, shown in Fig. 4(c), is a remarkably stable structure composed of seven localized peaks, each of which is similar to that of Fig. 4(a). Depending on the initial condition, we have also been able to find stable solutions with a few (typically two or three) centered hexagons far away from each other [see Fig. 4(d)]. Here again, we stress that the position of the centered hexagons depends on the initial conditions: they are stable against variations of their positions. The dependence of the localized structures and patterns on the initial condition is apparent in Fig. 4 where the four pictures differ only by the initial condition. Because of this fact, all maxima in Fig. 4 have the same value, though the widths of the peaks and the ringing [i.e., additional but smaller maxima as seen clearly in Figs. 1(b) and 1(c)] are reduced as the number of localized structures or patterns increases. Indeed, we have verified that within numerical accuracy the integral of X^2 over the transverse dimension(s) is constant. In terms of the complete 3D system, the localized structures correspond to filaments and the fact that their peak power is the same irrespec-

tive of their number and may be an asset for applications dealing with information processing.

Most useful discussions with M. Georgiou are gratefully acknowledged. This work has been supported in part by the Interuniversity Attraction Pole program of the Belgian government and by the Fonds National de la Recherche Scientifique.

[1] P. Mandel and T. Erneux, Opt. Commun. **44**, 55 (1982); for a complete linear stability analysis of optical bistability, see L. A. Lugiato and C. Oldano, Phys. Rev. A **37**, 3896 (1988).

[2] P. Mandel, M. Georgiou, and T. Erneux, Phys. Rev. A **47**, 4277 (1993).

[3] After submission of this paper, we received a preprint submitted to Physica D by L. Yu. Glebsky and L. M. Lerman entitled "On the small stationary self-localized solutions for generalized 1D Swift-Hohenberg equation," where the authors establish analytically the existence of small amplitude localized structures for a class of generalized 1D Swift-Hohenberg equations to which Eq. (2) belongs.

[4] S. Koga and Y. Kuramoto, Prog. Theor. Phys. **63**, 109 (1980); V. Hahim, P. Jakobsen, and Y. Pommeau, Europhys. Lett. **11**, 19 (1990); G. Dewel and P. Borckmans, in *Far from Equilibrium Dynamics of Chemical Systems*, edited by J. Popielawski and J. Gorecki (World Scientific, Singapore, 1991), p. 83.

[5] Sadayoshi Toh, Hiroshi Iwasaki, and Takuji Kawahara, Phys. Rev. A **40**, 5472 (1989); O. Thual and S. Fauve, J. Phys. (Paris) **49**, 1829 (1988); A. V. Gaponov-Grekhov, A. S. Lomov, G. V. Osipov, and M. I. Rabinovich, in *Nonlinear Waves*, edited by A. V. Gaponov-Grekhov, M. I. Rabinovich, and J. Engelbrecht (Springer, Heidelberg, 1989), Vol. 1, p. 65.

[6] G. S. McDonald and W. J. Firth, J. Opt. Soc. Am. B **7**, 1328 (1990).

[7] N. N. Rosanov and G. V. Khodova, J. Opt. Soc. Am. B **7**, 1057 (1990).

[8] D. W. McLaughlin, J. V. Moloney, and A. C. Newell, Phys. Rev. Lett. **51**, 75 (1983).

[9] P. Coullet and K. Emilson, Physica (Amsterdam) **61D**, 119 (1992).

[10] *Nonlinear Dynamics and Spatial Complexity in Optical Systems*, edited by R. G. Harrison and J. S. Uppal (Institute of Physics, Bristol, 1993).

[11] L. A. Lugiato and R. Lefever, Phys. Rev. Lett. **58**, 2209 (1987).

[12] P. Manneville, *Dissipative Structures and Weak Turbulence* (Academic, New York, 1990).

[13] M. Tlidi, M. Georgiou, and Paul Mandel, Phys. Rev. A **48**, 4605 (1993).

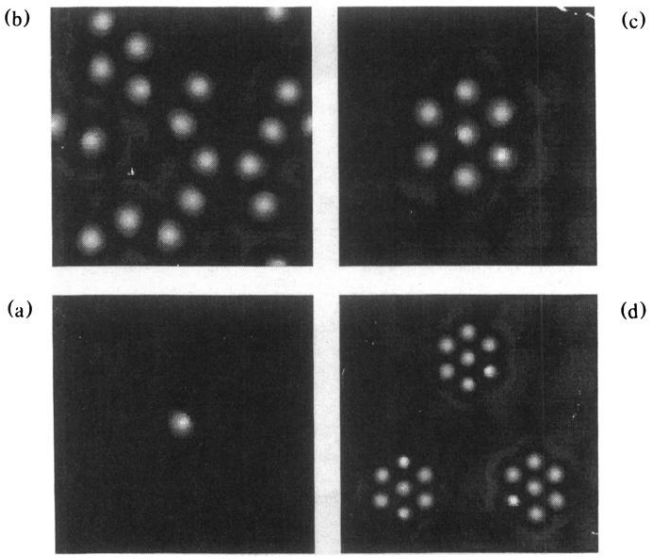

FIG. 4. Localized structures and patterns with two transverse dimensions ($\Delta = 0.1$, $\mathcal{C} = 0.025$, and $y = -0.0005$). (a) Single localized structure ($\Delta X = 5, 60 \times 60$ grid). (b) Random distribution of localized structures; the system is perturbed by small amplitude ($X = 0.92$, $\Delta X = 0.05$, 60×60 grid). (c) Localized pattern (centered hexagons). The steady state is perturbed at seven grid points. (d) Localized pattern (three centered hexagons, 100×100 grid).